Comparative transcriptome analysis reveals the late-acting self-incompatibility and identification of RNase T2 family members in Camellia oleifera

Chang Li[1,2‡], Mengqi Lu[1,2‡], Junqin Zhou [1,2*], Yi Long [1,2], Fuhao Zhang[3], Yan Xu[1,2], Nan Jiang[4], Xiaofeng Tan[1,2*]

[1]Key Laboratory of Cultivation and Protection for Non-Wood Forest Trees, Ministry of Education

[2]Central South University of Forestry and Technology, Changsha 410001, Hunan Province, China

[3]Anhui Agricultural University, Hefei 230000, Anhui Province, China

[4]Hunan University of Technology, Zhuzhou 412000, Hunan Province, China

* Correspondence: Junqin Zhou, zz_csuft@163.com; Xiaofeng Tan, tanxiaofengcn@126.com; Tel.: +86-0731-856-23406

‡These authors contributed equally to this work.

Abstract

Background: The Camellia oil tree (*Camellia oleifera* Abel.) is an important nonwood forest species in southern China, and most Camellia oil tree cultivars are late-acting self-incompatibility (LSI) types. Although several studies examined the mechanism of LSI, the process is quite complicated and unclear.

Result: The present study investigated pollen tube growth and fruit setting of two Camellia oil tree cultivars Huashuo (HS) and Huajin (HJ) after non- and self-pollination, and transcriptomic analysis of the ovaries was performed 48 h after self-pollination to identify the candidate genes involved in the LSI of Camellia oil tree. The results showed that the fruit set of HS after self-pollination was significantly higher than that of HJ. Transcriptomic analysis revealed that plant hormone signal transduction, ATP-binding cassette (ABC) transporters, the phosphatidylinositol signaling system, reactive oxygen species (ROS) metabolism, and Ca^{2+} signaling were mainly involved in the LSI of Camellia oil tree. Moreover, nine RNase T2 genes were identified from the transcriptome analysis, which also showed that CoRNase7 participated in the self-incompatibility reaction in HS. Based on phylogenetic analysis, *Co*RNase6 was closely related to S-RNase from coffee, and *Co*RNase7 and *Co*RNase8 were closely related to S-RNase from *Camellia sinensis*. The 9 RNase T2 genes successfully produced proteins in prokaryotes. Subcellular localization indicated that CoRNase1 and CoRNase5 were cytoplasmic proteins, while *Co*RNase7 was a plasma membrane protein.

Conclusions: These results preliminarily revealed the molecular mechanism of LSI in Camellia oil tree, and SI signal transduction might be regulated by a large molecular regulatory network. The discovery of T2 RNases provided evidence that Camellia oil tree might be under RNase-based gametophytic self-incompatibility.

Keywords: Camellia oil tree; Late-acting self-incompatibility; Transcriptome; RNase T2 family.

Background

Camellia oil tree (*Camellia oleifera*), an important member of the Camellia genus in the family Theaceae, is one of the most important broad-leaved evergreen tree species in southern China[1, 2]. This species has been cultivated for a long time (more than 2300 years)[3]. Because its seeds can be used to produce high-quality edible oil and because this species is widely cultivated, Camellia oil tree has become one of the world's four major woody edible oil tree species, together with oil palm (*Elaeis guineensis*), olive tree (*Olea europaea*), and coconut palm (*Cocos nucifera*)[4, 5]. Camellia oil is rich in unsaturated fatty acids, which account for more than 90% of the total seed oil, and is used as a high-grade edible oil known as 'oriental olive oil'[6, 7]. Camellia oil also contains many

active ingredients, such as triterpenes, vitamins, squalene, tocopherols, carotene, saponins, glycerol, and alcohol[8]. Consumption of large amounts of camellia oil can improve cardiovascular and cerebrovascular function and can lower cholesterol levels[9]. In *C. oleifera* production, self-incompatibility (SI) has always been an important factor limiting the yield of *C. oleifera*[10]. SI can also cause high heterogeneity within chromosomes, which hinders whole-genome sequence assembly and the construction of genetic maps of C. *oleifera*[11, 12]. Elucidating the molecular mechanism of SI is therefore important for the development of the camellia oil tree industry.

SI is a genetically controlled mechanism that prevents self-fertilization and facilitates outcrossing in flowering plants, which is beneficial for maintaining genetic diversity and resisting adverse environmental conditions[13]. SI is a widespread mechanism; more than half of all angiosperm species—more than 70 families and 250 genera—undergo SI[14, 15]. Although SI has been widely found in angiosperms, the molecular mechanism is derived from a small sample of just five families[15]. In general, SI systems in flowering plants can be classified into three main classes: sporophytic self-incompatibility (SSI), gametophytic self-incompatibility (GSI) and late-acting self-incompatibility (LSI)[16]. In SSI, the SI phenotype is determined by the diploid genotype of its anthers[17]. SI occurs when any one of the S genotypes in pollen from the anthers is the same as the S genotype of the pistils, and it is controlled by two main genes at the S locus: *S-receptor kinase* (SRK) (specifically expressed in the style) and the *S-locus cysteine-rich* (SCR) protein (specifically expressed in pollen). SI has been widely studied in *Cruciferae*. In GSI, the SI phenotype is defined by the gametophytic haploid genotype[17], and it is controlled by multiple alleles loci (S loci) of two combined factors called S-RNase genes and F-box genes, which are the female and male determinants of SI specificity, respectively[18–20]. There are many studies on female SI factors, and the cDNA of S-RNase, which is a type of RNase, has been extracted and cloned from pistils in many different species, such as *Malus domestica*, *Pyrus serotina* Rehd, *Citrus* and *Petunia* hybrids[21–24]. Another GSI mechanism exists in Papaveraceae species in which programmed cell death (PCD) of pollen tubes is induced by a Ca^{2+} signaling cascade[11].

LSI is categorized according to the location at which pollen tubes are inhibited, as pollen tubes resulting from self-pollination didnot reach the ovary; LSI was different from GSI and SSI, which were based on genetic mechanisms[16]. LSI has been reported in species of many diverse families, including *Ipomopsis aggregata* (Polemoniaceae), *Ceiba speciosa* (Bombacoideae), *Spathodea campanulata* (Bignoniaceae) and *Camellia sinensis* (Theaceae)[15, 25]. However, the genetic control of LSI has been investigated little and remains controversial[26]. Lipow demonstrated that LSI in *Asclepias exaltata* is regulated by a single locus with multiple alleles[27], whereas via transcriptome analysis, Zhang suggested that LSI of *C. sinensis* might be under gametophytic control [11]. PCD in SI is complex and likely regulated by a large network. Recently, researchers have focused on screening non-S factors and downstream signaling pathways involved in SI. Liwei et al. demonstrated that apple S-RNase could cause the accumulation of inorganic pyrophosphatase (Ppi), which inhibited tRNA aminoacylation and resulted in a reduction in pollen growth[28]. Reactive oxygen species (ROS) could act as secondary signaling molecules that play an important role in pollen tube growth, and self-PrsS in poppy pollen tubes increased the ROS content in a calcium-dependent manner[29, 30]. In apple, cytoplasmic Ca^{2+} concentrations and Ca^{2+} signaling cascades led to downstream depolymerization of actin filaments (AFs), pollen tube tip growth arrest and, consequently, PCD[20]. It had also been reported that S-RNase activity in the pollen tube caused changes in phospholipases[31]. Because the male determinants of SI had not been determined, research on *C. oleifera* SI tends to be slow. A previous study indicated that *C. o*leifera presented the characteristics of LSI[8], but the underlying molecular mechanism is still

unclear. Theself-incompatible of *C. oleifera* varieties had been found, and studies of self-incompatibility in *Camellia oleifera* were based on self- and cross-pollination. Few studies have focused on compatibility differences across varieties. Our study investigated differences in the inbreeding affinity of two *C. oleifera* cultivars using transcriptome analysis to reveal the main pathway involved in LSI-based non- and self-pollination, we identified a candidate S-RNase within the RNA sequencing (RNA-seq) data from the ovaries at 48 h after self-pollination. We also evaluated another 8 RNase T2 genes that were identified in the transcriptome and expressed in the ovaries. To identify more candidate S genes associated with LSI in *C. oleifera*, we cloned these 9 RNases, and sequence phylogenetic, gene structure, prokaryotic expression, and subcellular localization analyses were performed to distinguish S-RNases from other members of RNase T2family. The results should help elucidate the mechanism of LSI in Camellia oil trees, which will provide a theoretical foundation for the production and cultivation of *C. oleifera*.

Results

Determination of the occurrence of SI and fruit set evaluation

Flower buds at the large bud stage were selected for self-pollination (Figure 1A and C). Fluorescence microscopy observations demonstrated that pollen grains from both Huashuo (HS) and Huajin (HJ) germinated successfully after self-pollination, and no obvious differences were observed in the rate of elongation of the pollen tubes. At 24 h after self-pollination, the pollen tube of HJ had almost arrived at the middle position of the style channel, which was faster than that of HS (Figure 1B and D). The pollen tubes of both cultivars arrived at the style base at 48 h after self-pollination, and afterward, the pollen tubes grew more slowly and stopped at the base of the styles, failing to penetrate the ovaries to complete double fertilization. These results are consistent with those of previous research[8]. Thus, we determined that the SI of HJ and HS occurs between the base of the style and the upper ovary, and the SI occurred at 48 h after self-pollination. In addition, we found that a few pollen tubes could penetrate the style and reach the micropyle and complete double fertilization, which was similar to the processes involving cross-pollination (Figure 1E-F). At two months after self-pollination, the fruit sets were investigated. We found that the fruit setting percentages of HS was 34.20%, which was significantly higher than in HJ (19.14%) (Figure 1F). The observation and investigation support that *C. oleifera* is a late-acting self-incompatibility plant, and there are differences in the degree of self-incompatibility in different varities of *C.Oleifera*.

Transcriptome assembly and function annotation

Based on fluorescence microscopy observations of pollen tube growth, the transcriptomes of HJSP and HSSP at 48 h after self-pollination were compared with HJNP and HSNP without pollination. Twelve RNA-seq libraries were separately constructed by high-throughput sequencing. In total, 54.59~65.74 million reads of raw sequence data were obtained, and an average of approximately 58.90 million clean reads for each sample were obtained after being quality filtered. The Q30 was more than 94.01% for each sample, and the GC content ranged from 43.08% to 43.39%. Approximately 91.67% of the clean reads were totally mapped to the reference genome of Camellia oil tea (Table 1). About 15,091 unannotated unigenes were found (Supplementary table S1), and 12,911 of these genes were annotated after blasted with four databases, with 12,911 unigenes in NCBI non-redundant protein sequence (NR) database, 7,462 in Swiss-Prot Protein Database (Swiss-Prot), 6,597 in Gene Ontology (GO) database, and 2,874 in Kyoto Encyclopedia of Genes and Genomes (KEGG) database.

Comparative analysis of differentially expressed genes (DEGs)

To identify the DEGs related to the LSI of Camellia oil tea, fragments per kilobase of transcript per million mapped reads (FPKM) were used to measure the expression level of the unigenes. In total, 5,082 and 4,277 DEGs

were detected in the HJNP_HJSP and HSNP_HSSP comparisons, 3,730 upregulated and 1,352 downregulated genes were identified in the HJNP_HJSP comparison, 2,881 upregulated and 1,396 downregulated genes were identified in the HSSP_HSNP comparison (Figure 2A), and 1,740 common DEGs (1,378 commonly upregulated and 339 commonly downregulated) were expressed in all the comparison groups (Figure 2B). These findings suggested that these 1,740 DEGs might be involved in the LSI of the Camellia oil tree.

GO and KEGG pathway analysis of DEGs

To assess whether the DEGs have any significantly functional enrichment, GO term enrichment analyses were performed. Among them, the top four GO terms in the biological process category were 'metabolic process', 'cellular process', 'single-organism process' and 'response to stimulus'; the top four GO terms in the molecular function category were 'catalytic activity', 'binding', 'transporter activity' and 'nucleic binding transcription factor activity'; and the top four GO terms in the cellular component category were 'cell', 'cell part', 'organelle' and 'membrane' (Figure 2C).

KEGG pathway analysis indicated that 123 pathways were enriched in the HJNP_HJSP gene set and 118 pathways were enriched in the HSNP_HSSP gene set. All of the pathways from the two comparison groups could be divided into five categories: metabolism, genetic information processing, environmental information processing, cellular process and organismal systems. The top 15 significantly enriched pathways of the two comparison groups are listed in Figure 3A-B. The major enriched pathways that might be related to SI were identified in both the HJNP_HJSP gene set and the HSNP_HSSP gene set: plant hormone signal transduction (ko04075), phosphatidylinositol signaling system (ko04070), ATP-binding cassette (ABC) transporters (ko02010), MAPK signaling pathway-plant (ko04016), plant–pathogen interaction (ko04626), flavonoid biosynthesis (ko00941), and ubiquitin-mediated proteolysis (ko04120). Among them, plant hormone signal transduction (ko04075), ABC transporters (ko02010), biosynthesis of secondary metabolites (ko01110), and phenylpropanoid biosynthesis (ko00940) were among the top 10 significantly enriched pathways (Figure 3A-B).

DEGs related to plant hormone signal transduction

Plant hormone signals are involved in regulating plant physiological and biochemical processes to a large extent, including pollen–stigma interactions, seed germination and development, pollen tube polar growth and so forth[32–34]. In this study, we identified 112 DEGs in the HJNP_HJSP gene set and 102 DEGs in the HSNP_HSSP gene set. Among them, 54 DEGs were related to plant hormone signal transduction pathways, which included some involved in cytokine (CK), abscisic acid (ABA), gibberellin (GA), and jasmonic acid (JA) pathways were significantly expressed in the two comparison groups. The histidine-containing phosphotransfer protein gene (AHP), the two-component response regulator ARR-B family (ARR-B) and the two-component response regulator ARR-A family (ARR-A) were upregulated in the CK pathway of both groups. The histidine-containing phosphotransfer protein gene (AHP) was also upregulated in the HJNP_HJSP gene set, but there was no significant difference in the HJNP_HJSP gene set. In the ABA signaling pathway, the ABA receptor PYL1-like gene (*PYL1*) was downregulated in the HJNP_HJSP gene set and was not significantly different in the HSNP_HJSP gene set. In the GA signaling pathway, the phytochrome-interacting factor 3 gene (PIF3) and the gibberellin receptor GID1 gene (GID1) were upregulated in the two comparison groups, and GID2 was downregulated in HJSP compared to HJNP. The transcription factor MYC2-like (MYC2) and jasmonic acid-amino synthetase (JAR1) were upregulated in the JA signaling pathway of both comparison groups (Figure 3C), and jasmonate ZIM domain-containing protein (JAZ) was downregulated in both comparison groups. Taken together, these results indicated that plant hormone signal

transduction pathways might play important roles in the LSI of Camellia oil trees.

DEGs involved in ABC transporters

ABC transporter proteins compose a large class of transmembrane proteins that transport substrates across the lipid bilayer of the cell membrane mainly through the energy produced by the hydrolysis of ATP. It had been demonstrated that the transport of S-RNase was mediated by ABCF[35]. In this study, the DEGs in both groups were significantly enriched in ABC transporters. In the HJNP_HJSP gene set, there were 36 DEGs encoding proteins related to ABC transporters, namely, 9 *CoABCB*, 21 *CoABCC*, and 6 *CoABCG* genes. *CoABCC10* was the major gene upregulated in HJSP, while the 6 *CoABCG* genes were downregulated in HJ after self-pollination. In the HSNP_HSSP gene set, there were 24 DEG-encoding proteins related to ABC transporters, namely, 6 *CoABCB* and 18 *CoABCC* genes. All 24 DEGs were significantly upregulated, but seventeen DEGs were significantly differentially upregulated in the two groups, namely, 6 *CoABCB* and 11 *CoABCC* (Figure 4c and Supplementary table S2). The results indicated that *CoABCB* and *CoABCC* might be involved in the LSI of Camellia oil tree.

DEGs related to the phosphatidylinositol signaling system

External stimulation can accelerate the metabolic activity of plant membrane lipids. Lnositol phospholipid compounds on the cell membrane are important secondary messengers in plant signal transduction. The current study revealed 7 DEGs (6 up-regulated and 1 down-regulated genes) in the HJNP_HJSP gene set and 10 DEGs (8 up-regulated and 2 downregulated genes) in the HSNP_HSSP gene set, which were involved in the phosphatidylinositol signaling system (Figure 4B and Supplementary table S3). In the HJNP_HJSP gene set, the phosphatidylinositol 4-phosphate 5-kinase 6-like (*PIP5K6*), diacylglycerol kinase 1-like isoform X2 (*DGK1*), and phosphoinositide phospholipase C 6-like (*PLC6*) genes were upregulated in the HJNP_HJSP gene set, while the diacylglycerol kinase 2 (*DGK2*) gene was downregulated. In the HSNP_HSSP gene set, the 1-phosphatidylinositol-3-phosphate 5-kinase (*PIP5K6*), FAB1B-like isoform X1 (*FAB1B*), inositol-pentakisphosphate 2-kinase-like isoform X2 (*IPK1*), inositol hexakisphosphate, diphosphoinositol-pentakisphosphate kinase VIP2-like (*VIP2*), and PLC6 genes were upregulated in HSSP compared with HSNP, while the phosphoinositide phospholipase C 2-like (PLC2) gene was downregulated. Comparing the two groups, we found that there were more types of DEGs in the HSSP group, and PLC6 was upregulated in both HSSP and HJSP.

DEGs related to ROS and the Ca^{2+} signaling pathway

Many studies have demonstrated that ROS play a key role in signal transduction in pollen tube polar growth and in the SI of *Papaver* and *Prunus avium*[36, 37]. When SI occurs, ROS levels in the pollen tube increased rapidly for [38] gene set, six *colRBOH* genes, three glutathione S-transferase (*colGST*) genes and three glutathione peroxidase (*colGPX2*) genes, all of which were involved in ROS scavenging, and six receptor-like protein kinase FERONIA (*colFER*) genes were upregulated in HJSP compared with HJNP. In the HSNP_HSSP gene set, four respiratory burst oxidase protein-like (*RBOH*) genes, one glutathione S-transferase U7-like (*GSTU7*) gene, two mitochondrial alternative oxidase 1d (*AOX1A*) genes and five receptor-like protein kinase HERK 1 isoform (*FER*) genes were upregulated. Overall, these results suggest that ROS might play an important role in the LSI of camellia oil tree, and the DEGs mentioned above might play an important role in balancing ROS production and scavenging.

As a secondary messenger, Ca^{2+} plays an important role in regulating pollen germination and preventing self-fertilization, and several DEGs related to Ca^{2+} signaling-related genes were identified in this study. Calcium-dependent protein kinase (*CDPK*) is an important primary sensory receptor for calcium signaling and is located at the top of pollen tubes[38]. One predicted *CDPK* has a high expression level in HJSP. Ca^{2+} outflow requires the

ACA and *CCX*, which can provide energy. Five calcium-transporting ATPase (ACA) genes and five cation/calcium exchanger 1-like (CCX) genes were upregulated in the HJNP_HJSP gene set. Similarly, four calmodulin-binding protein (*CAM*)-encoding genes were upregulated in the HSNP_HSSP gene set (Figure 4A and B).

A putative S-RNase gene involved in SI of *C. oleifera*

S-RNase-mediated SI widely exists in Solanaceae, Scrophulariaceae, and Rosaceae species[39, 40], and it is an important and widespread mechanism that prevents self-fertilization and promotes cross-pollination in plants. S-RNase belongs to the RNase T2 family, These types of genes can be divided into three groups according to their number of introns and phylogenetic relationships: S-like RNases include groups I and II, while S-RNases are assigned to group III[41]. In this study, a DEG encoding extracellular ribonuclease LE-like isoform X1 (*RNS1*), which is highly homologous to RNase genes, was most highly expressed in the HSNP_HSSP gene set.

Identification and characterization of T2 RNases in Camellia oil tree

In this study, We identified a total of 9 RNase T2 genes in *C. oleifera*, named *CoRNS1*, *CoRNS2*, *CoRNS3*, *CoRNS4*, *CoRNS5 CoRNS6*, *CoRNS7*, *CoRNS8*, and *CoRNS9*. The length of the coding DNA sequence (CDS) ranged from 429 to 789 bp, and the number of amino acids ranged from 143 to 315. The typical molecular weight of RNase T2 enzymes usually ranges from 25 to 32 kDa[42]. The molecular weights of 5 of the proteins encoded by the abovementioned gene were in this range, but those of the proteins encoded by *CoRNS2*, *CoRNS3*, *CoRNS4*, and *CoRNS9* were outside that range (15.65~17.39 kDa). The theoretical pI of the proteins encoded by these 9 genes ranged from 4.94~8.77. There were 6 acidic pI values and 2 basic pI values of these putative RNase T2 proteins. The signal peptide of the candidate RNase proteins in the pistil of *C. oleifera* was predicted by an online website, and the results showed that most RNase T2 proteins, except for *CoRNS4* and *CoRNS5*, contained signal peptides (Table 2). Multiple alignment of the amino acid sequences of the nine proteins and five other S-RNases clearly revealed similarities among Rosaceae species (Figure 5A). The results indicated that CoRNS1, CoRNS6, CoRNS7, and CoRNS8 contained conserved active sites named CAS I and CAS II, whose histidine residues are required for RNase T2 protein activity[43], while CoRNS1 and CoRNS6 have only one active site.

We could divide the RNase T2s into the S-RNase and S-like RNase categories according to the biological function of the RNases[44]. S-RNases are specifically expressed in flowering plants to regulate plant SI, and S-like RNases are mainly involved in responses to biotic and abiotic stress, such as antimicrobial defense, phosphate scavenging, the enhancement of stress tolerance and tRNA cleavage[45]. S-RNases and S-like RNases can also be classified into three groups: class I, class II, and class III. S-like RNases correspond to classes I and II, and S-RNases correspond to class III[43]. To better understand the exact classification of the RNase T2 genes in Camellia oil tree, a phylogenetic tree was constructed based on the sequences of our 9 RNase T2 proteins and another 15 annotated S-like RNases and 21 S-RNase proteins randomly retrieved from the protein database. The tree was constructed with the neighbor-joining (NJ) method using MEGA 7.0 and included monocotyledonous plant species such as rice, wheat, and corn and dicotyledonous plant species such as apple, pear, and coffee (Supplementary table S4). As shown in Figure 5B, all of the sequences were divided into three groups based on the characteristics of their protein structure, and *Co*RNase6 clustered on the same small branch as the S-RNase from coffee. This small branch clustered with a large branch consisting of annotated S-RNases from Rosaceae and Solanaceae. Another branch contained *Co*RNase1, *Co*RNase2, *Co*RNase3, *Co*RNase4, *Co*RNase5, *Co*RNase9 and 14 other S-like RNases that were identified. Interestingly, *Co*RNase7 and *Co*RNase8 were closely related to an S-RNase from *C. sinensis*, and *Co*RNase7 was identified as a DEG in the transcriptome of HSSP compared with HSNP. In addition, the proteins

on this small branch were more closely related to S-like RNases than to S-RNases. Taken together, these results indicated that *Co*RNase6, *Co*RNase7, and *Co*RNase8 were likely involved in SI, but the biological functions of the 9 proteins need to be further studied.

Prokaryotic expression analysis of RNases

Based on the principle of homologous recombination, 9 his-*Co*RNase recombinant expression vectors corresponding to the 9 RNase T2 genes were constructed and transformed into *Escherichia coli* Rosetta (DE3) for recombinant protein induction and expression. The 9 his-*Co*RNases were successfully induced in response to isopropyl β-D-1-thiogalactopyranoside (IPTG) at concentrations of 0, 0.5, 0.8, 1.0, 1.2, 1.4 and 1.6 mmol/L. The resulting protein sizes ranged from 73~90 kDa. These results indicated that the his-*Co*RNase prokaryotic expression vectors were successfully constructed and that the target proteins were successfully expressed in response to the induction of IPTG (Figure 6A and Supplementary Figure S1). With increasing IPTG concentration, the protein expression increased slightly or did not change to a large degree.

Subcellular localization of RNases

According to predictions from online sites, *Co*RNase8 from the Camellia oil tree was predicted to be localized in the cytosol, *Co*RNase5 was predicted to be localized in the nucleus, and the resident RNase localized to the extracellular space. To verify this, the *Co*RNase1, *Co*RNase5 and *Co*RNase7 genes were fused to green fluorescent protein (GFP), and the three GFP-fusion proteins were transiently expressed in leaves of *Nicotiana benthamiana*, as illustrated in Figure 6B. The green fluorescence of *Co*RNase1 and *Co*RNase5 was visible in the cytoplasm, and the green fluorescence of *Co*RNase7 was exclusively restricted to the plasma membrane. After treatment with NaCl solution, the tobacco cytoplasm was obviously separated from the cell wall, and the green fluorescence became concentrated (Figure 7B). Taken together, these results indicated that *Co*RNase1 and *Co*RNase7 were cytoplasmic proteins, while *Co*RNase5 was a plasma membrane-localized protein.

Quantitative real-time PCR (qRT–PCR) validation

To determine the reliability of the RNA-seq data, 12 DEGs involved in SI during SP and NP were chosen as targets based on their expression fold changes and FPKM, and *CoGAPDH* was chosen as an internal control and verified via qRT–PCR. The RNA-seq and qRT–PCR data were then compared. As Figure 8 shows, the change trend of these DEGs in the four samples according to the qRT–PCR results was highly similar to that of the transcriptomic data sets. This means that the data obtained from RNA-seq were reliable.

Discussion

Camellia oil tree (*C. oleifera* L.) is the most important edible oil tree species in southern China. Camellia oil is rich in unsaturated fatty acids such as oleic acid and linoleic acid and contains important health components such as squalene and sterol[46]. However, oilseed yields are low under natural conditions, and LSI is one of the key factors limiting the production of camellia oil trees[25].

LSI is a specific SI system that has been found in many plant species, but the molecular mechanism underlying this phenomenon in Theaceae species is still unclear[8]. Fluorescence microscopy observations demonstrated that pollen tubes resulting from self-pollination could grow to the bottom of the style but then stopped in both *C. oleifera* HS and *C. oleifera* HJ, and similar findings were found in Cacao and *C. sinensis*[11, 26]. Furthermore, to better understand the molecular mechanism of LSI in camellia oil tree, transcriptomic analysis of the ovaries of the two camellia oil tree cultivars was performed. The results revealed large complex regulatory networks involved in the LSI process, mainly including ABC transporters, plant hormone signal transduction, ROS, Ca^{2+},

phosphatidylinositol signaling and S-RNases, which are discussed below.

Plant hormone signal transduction related to the SI of the two cultivars of *C. oleifera*

Phytohormones, such as auxin (IAA), ethylene (ET), CKs, GA, brassinosteroids (BRs), ABA, salicylic acid (SA), and JA, are small signaling molecules that play an important role in regulating plant endogenous developmental processes and responses to environmental stress[47–49]. Many studies have reported that phytohormones play important roles in plant SI[50, 51]. In this study, DEGs were significantly enriched in plant hormone signal transduction pathways in the ovaries of self-pollinated *C. oleifera* HJ and HS.

GID1 is a receptor of GA, and the DELLA protein is a plant growth repressor. GA, GID1 and DELLA form a complex triggered by GAs, which forms ubiquitinated DELLA, and the plant growth suppressor may be dismissed once DELLA is degraded by the 26S protein[34]. Previous research found that the content of endogenous GA in the pistils of pear increased after pollination, but when the pollen tube stopped growing due to self-incompatibility, the content of endogenous GA in the pistil decreased, which was also found in apple[52]. In this study, we found that PIF3 and GID1, which positively regulate the GA response in both cultivars of *C. oleifera*, were upregulated in the two comparison groups. JA plays an important role in the plant defense response. Gu[53] found that S-RNase in pollen tubes could promote an increase in JA content in self-pollinated flowers. Here, we found that MYC2, a positive regulatory transcription factor in the JA signaling pathway, was upregulated in both groups. ABA plays an important role in the plant stress response, flower bud induction, seed dormancy and germination[54–56], and it can induce the synthesis of S-RNase involved in pear SI[34]. As a negative regulator of self-pollination, *PYR/PYL* was downregulated in the ovaries of *C. oleifera* HJ. These results were consistent with those of previous reports on cacao, whose ABA components were increased in flowers after self-pollination[57], which suggested that the ABA signaling cascade participated in the pistil response to pollen, and CK plays an important role in cell division, seed germination and plant–pathogen interaction[58]. The content of CK increased five-fold in *petunia hybrid* plants when pollen tube growth was inhibited[34]. Genes related to CK signal transduction, including CRE1, AHP, B-ARR and A-ARR, were upregulated in both comparison groups in our study. Our previous study found that the ZR content in pistils showed a slow upward trend within 24-48 after self-pollination in *C. oleifera*. These results suggest that CK participates in pollen discrimination and plays an important role in the LSI reaction in camellia oil trees. Taken together, the results indicate that the plant hormone signaling pathway participates in the LSI of *C. oleifera*.

ABC transporters related to the SI of the two cultivars of *C. oleifera*

ABC transporters constitute a large family of transmembrane transport proteins in plants, and the main function of these proteins is to transport multiple types of substrates across the plasma membrane via ATP hydrolysis[59, 60] for toxin enrichment and efflux, maintenance of cellular osmotic homeostasis and stomatal movement in response to environmental stress. ABC transporters are also important in seed germination and root development[59]. A previous study in *M. domestica* demonstrated that *MdABCF* in pollen could combine with S-RNase, a key protein of GSI, and transport it to the cytoplasm of the pollen tube to facilitate its cellular cytotoxic function[35]. In the present study, DEGs were significantly enriched in ABC transporters. Twenty-six DEGs, namely, 6 *CoABCB*s and 20 *CoABCC*s, were highly expressed in the HJNP_HJSP gene set. Similarly, 22 DEGs, namely, 4 *CoABCB*s and 18 *CoABCC*s, were highly expressed in the HSNP_HSSP gene set, and 14 were commonly upregulated. Taken together, these results indicate that *CoABCB* and *CoABCC* might participate in the LSI of *C. Oleifera*.

Phosphatidylinositol signaling system related to the SI of the two cultivars of *C. oleifera*

When cells receive various external or internal signals, the organisms respond with corresponding

physiological effects, and the phosphatidylinositol signaling system is among the most universal molecular reaction mechanisms involved in signal transduction. The inositol phosphate compounds IP3 and DAG on the cell membrane are secondary messengers in plant signal transduction pathways[61]. Phospholipase C (PLC) also plays an important role in phosphatidylinositol (4,5) P_2 hydrolysis, and the downstream product phosphatidic acid (PA) can mitigate PbrS-RNase cytotoxicity to protect the pollen tube[28]. In the current study, the phosphatidylinositol signaling system showed significant enrichment in DEGs in the ovary transcriptome during SI, among which the *PLC6* gene was upregulated in both the HJNP_HJSP gene set and the HSNP_HSSP gene set. We assume that overexpression of *PLC6* might contribute to the hydrolysis of phosphatidylinositol and trigger complex protective mechanisms against environmental stimuli and harm. IPK, which is a positive factor in the phosphatidylinositol signaling pathway, was upregulated in HSSP compared to HSNP. IPK regulates root and pollen tube growth in Arabidopsis in a calcium-dependent manner[62]. Taken together, the DEGs encoded proteins or enzymes related to the phosphatidylinositol signaling system, which may be involved in the response to the LSI of the Camellia oil tree.

ROS and Ca^{2+} related to the SI of the two cultivars of *C. oleifera*

When they are present in excessive amounts, ROS have been described as toxic metabolic products[63–65], but they can also act as secondary signaling molecules in response to biotic and abiotic stresses and can trigger different types of PCD in normal plant development[66]. Many studies have confirmed that ROS participate in flower development and many pollen-related processes, such as in vitro pollen germination[67], the growth process of the pollen tube apex[68], stigma and pollen recognition and SI[69]. In the current study, we found 19 DEGs that were involved in ROS metabolism in the HSSP_HSNP gene set and 16 DEGs in the HJNP_HJSP gene set. These DEGs included *RBOH*, *GPX2*, *FER*, *GST*, and *GSTU7*. In addition, RBOH during both self- and non-pollination was upregulated. We previously found that the content of ROS in plants showed a significant upward trend at 12-48 h after self-pollination and peaked at 48 h, and respiratory burst oxidases (*RBOHs*) were shown to play a key role in ROS generation[64]. This means that ROS function in plant defense during this time. In poppy, PrsS in the pollen tube could cause an increase in ROS triggered by calcium-dependent proteins[66]. In *Pyrus*, the ROS position in the tip of the pollen tube can be disrupted by self-S-RNase[70]. Our study suggested that ROS might directly be involved in the LSI process of *C. oleifera*.

DEGs related to Ca^{2+} signaling were also identified in this study. Ca^{2+} plays an important role in pollen tube growth and has a vital function in SI[71, 72]. It was reported that IP_3 could act on IP_3 receptors on the endoplasmic reticulum and cause Ca^{2+} channel opening and Ca^{2+} release. In addition, Ca^{2+} can promote the production of ROS during pollen tube tip growth[36] (Figure 5A). Ca^{2+} signaling cascades could lead to PCD in Papaveraceae, which is part of the GSI mechanism[73]. In *petunia*, overexpression of the Ca^{2+} response element (Pi *CDPK1* and Pi *CDPK2*) could restrict extension of the pollen tube or disrupt the polarity of tube growth [38]. These results indicated that the phosphatidylinositol signaling system might be involved in the SI of Camellia oil tree through the Ca^{2+} signaling cascade. In the current study, we found that the expression of three CaM genes was significantly upregulated in the two groups. Taken together, these results indicated that Ca^{2+} signaling-related genes may be involved in the LSI of *C. oleifera*.

S-RNase related to the SI of *C. oleifera*

S-RNases have been demonstrated to be female determinant genes involved in the rejection of self-produced pollen and causing GSI in plants of the Solanaceae, Scrophulariaceae and Rosaceae families[74–76]. The Camellia oil tree was identified as undergoing LSI according to the location at which pollen tube growth was inhibited instead

of the genetic mechanism, and the molecular mechanism of LSI is still unclear. In this study, a putative S-RNase gene was found that was significantly upregulated in the HSNP_HSSP gene set, and another eight genes highly homologous to T2 RNase were cloned. These nine T2 RNases successfully expressed proteins in prokaryotes. Zhang[11] found an S-RNase gene that was highly expressed in a style that was self-pollinated vs. one that was cross-pollinated at 24 h post-pollination in tea (*C. sinensis* L.), which is in the same family as the Camellia oil tree (Theaceae family). Both were under LSI because the pollen tubes resulting from self-pollination were inhibited in the ovaries[77]. Taken together, these results indicate that the LSI of Camellia oil tree might be based on GSI.

RNase T2 family members in *C. oleifera*

We identified *9 RNase T2* genes based on the transcriptome data of *C. oleifera*. It was determined via multiple sequence alignments that most of the RNase T2 proteins (except *CoRNS5* and *CoRNS9*) contained conserved histidine active sites. *CoRNS6* was assigned to the *S-RNase* class according to phylogenetic analysis, and *CoRNS7, CoRNS8* and another S gene identified in *C. sinensis* clustered onto the same small branch. Prokaryotic expression analysis indicated that these 9 proteins were successfully expressed, and subcellular localization indicated that *Co*RNase1 and *Co*RNase5 were cytoplasmic proteins, while *Co*RNase7 was a plasma membrane-localized protein. Thus, S-RNases and S-like RNases in camellia oil tree could be distinguished preliminarily based on the results of these analyses, and we will continue to conduct further functional research on these genes.

Materials and methods

Plant materials, pollination treatment and sample collection

Two SI camellia oil tree varieties, Huajin (HJ) and Huashuo (HS), were selected in this study. The two cultivars(No voucher specimen) were selected for a comparative regional assessment out of 84 *C.oleifera* clones, it was identified by professor Tan Xiaofeng and Yuan Deyi from Central South University of Forestry and Technology, and named by the Forest Variety Committee of the State Forestry Administration[1, 78, 79], they are cultivated at the Huju Forest Farm in the Chaling district, Zhuzhou city, Hunan Province, China (26°47’24’ N, 113°32’24’ E). The peak flowering period of HJ occurred at the end of October, while that of HS was at the beginning of December. The growth and the number of flowers produced by these two cultivars were otherwise normal.

The anthers were collected from mature buds of two cultivars HJ and HS. Then the anthers were placed at 25°C room temperature for 8 h, and the pollen were gathered after anther scattering. Four pollination treatments were designed: HJ×HJ (HJSP), HS×HS (HSSP), non-pollination of HJ (HJNP) and non-pollination of HS (HSNP). Pollination was performed from 8:00-11:00 am and from 1:00-5:00 pm on sunny days in late October and early December. The flowers were emasculated and pollinated according to the four pollination treatments. Then all treated materials were wrapped in a sulfate paper bag. At 48 h after pollination, the ovaries for RNA-seq and qRT–PCR were collected and stored at −80°C (3 biological replicates), and each replicates comprised 50 ovaries. The pistils for pollen tube observations were collected at different intervals (0, 12, 24, 36, 48, 60, 72, 84 h) and then fixed with Carnoy’s fixative.

Data surveys and cytological observations

After removing the pistils from Carnoy’s fixative, the pistils were macerated in sodium hypochlorite for softening. After they were incubated for 2 hours at room temperature, the pistils were rinsed with deionized water and then macerated in 8 M NaOH for 2 h. Then, the styles were split along the vertical axis into 3-5 sections with a surgical blade and stained with aniline blue for 6 h. Finally, pollen tube growth was observed using fluorescence microscopy.

RNA-seq, transcriptome assembly and functional annotations

RNA samples were sent to Gene Denovo Biotechnology Co. (Guangzhou, China). The libraries were constructed and sequenced. Total RNA was extracted using TRIzol reagent (Invitrogen, Carlsbad, CA, USA) according to the manufacturer's protocol. The rRNA was subsequently removed using a Ribo-Zero^{TM} Magnetic Kit (Epicenter, Madison, WI, USA). Then, the enriched mRNA was fragmented into short pieces using fragmentation buffer and reverse transcribed into cDNA with random primers. Second-strand cDNA was synthesized by DNA polymerase I, RNase H, dNTPs and buffer. Then, the cDNA fragments were purified with a QIAquick PCR extraction kit (Qiagen, Venlo, The Netherlands), end repaired, polyadenylated, and ligated to Illumina sequencing adapters. The ligation products were subjected to size selection via agarose gel electrophoresis, amplified via PCR, and sequenced using an Illumina NovaSeq 6000.

Reads obtained from the sequencing machines included raw reads, which affected the subsequent assembly and analysis. To obtain high-quality clean reads, the reads were further filtered by fastp[80], and rRNA sequences were removed by alignment. The genome data of *Camellia oleifera*'Huashuo' has been obtained (the paper has not yet been published). An index of the reference genome was built, and paired-end clean reads were mapped to the reference genome using HISAT 2.2.4[81] with "-rna-strandness RF" and other parameters set as a default. The mapped reads of each sample were assembled by using StringTie v1.3.1[82, 83] in a reference-based approach. The unannotated transcripts were blasted to the four databases including: NR, Swiss-Prot, GO and KEGG databases [84]. RNA differential expression analysis was performed by DESeq2[85] software between the two different groups (and by edgeR [86] between two samples).

Gene cloning, multiple sequence alignment and phylogenetic analysis

Based on the transcriptomic data, the full-length CDSs of 9 RNase T2 family genes were obtained. The corresponding 9 pairs of primers were designed by Primer Premier 5.0 and synthesized by Shanghai Shenggong Bioengineering Co. (Shanghai, China). The cDNA of ovary in Camellia oil tree HS was used as a template, and the 9 RNase T2 genes were cloned. Target gene fragments were detected via gel electrophoresis and recovered by a gel recovery kit. The recovered target fragments were subsequently ligated into a pUC19 vector, which was then transformed into *E. coli* DH5α. Bacteria exhibiting good growth were selected and sequenced. The amino acid sequences of the 9 RNase T2 genes were blasted and aligned using NCBI and DNAMAN, respectively.

To divide these 9 RNase T2 genes into two categories, S-RNases and S-like RNases, a phylogenetic tree was constructed using the neighbor-joining (NJ) method by MEGA 7.0. The phylogenetic tree contained 9 candidate RNase proteins of Camellia oil tree and 36 RNase T2 enzymes reported for different species. Those data were downloaded from the UniProt database (http://www.uniprot.org/)

Recombinant protein expression

To analyze the subcellular localization of the 9 *CoRNase* genes, leaves of *N. benthamiana* were infected with GV3101 containing CoRNase:GFP, cultured for 48 h, and then observed by an LSM 510 laser confocal microscope. The excitation wavelength used to detect GFP was 488 nm, and the emission wavelength was 495-545 nm.

To ensure that these 9 CoRNases could be successfully expressed as proteins and for subsequent experiments, the CoRNases proteins without signal peptides were fused to His-tag. The recombinant protein was expressed in *E. coli* strain BL21 (DE3) (QINGKE) and induced by IPTG at different concentrations (0, 0.5, 0.8, 1.0, 1.2, 1.4, 1.6 mM).

qRT–PCR verification

To verify the accuracy of the RNA-seq data, a total of 9 DEGs related to LSI of Camellia oil tree were selected and evaluated by qRT–PCR (Supplementary Table S4). The RNA of those samples was extracted by a plant RNA kit (OMEGA, USA), and the remaining elimination of potential gDNA and reverse transcription were performed with HiScript® II Q RT SuperMix for qPCR (+gDNA wiper) (Vazyme, Nanjing, China). Specific primers for the 9 DEGs were designed by Primer Premier 5.0 (Supplementary Table S4). QRT-PCR was conducted in conjunction with ChamQ Universal SYBR qPCR Master Mix #Q711 (Vazyme, Nanjing, China). This experiment was performed on a CFX96 Real Time PCR System (Bio-Rad, Hercules, CA, USA), and *CoGAPDH* was chosen as the reference gene for Camellia oil tree. The expression level of the target gene was calculated with the $2^{-\Delta\Delta CT}$ method. Each sample was analyzed in triplicate.

Declarations

Ethics approval and consent to participate

All experiment materials were collected complied with the IUCN Policy Statement on Research Involving Species at Risk of Extinctionand the Convention on the Trade in Endangered Species of Wild Fauna and Flora.

Consent for publication

Not applicable

Availability of data and material

All data generated or analyzed during this study were included in this published article and the additional files. The RNA-seq data can be found in SRA data library under accession number PRJNA867027. https://dataview.ncbi.nlm.nih.gov/object/PRJNA867027?reviewer=a52f1c6obqs98rp0uio5a346db

Competing interests

The authors declare no conflicts of interest.

Funding

This study was funded by the National Natural Science Foundation of China (Grant number 31730016).

Authors' contributions

Methodology, C.L., J.Z. and X.T.; data investigation, C.L., M.L. and Y. L; data curation, L.Y.; Resources, Y.L. F.Z. and Y.X.; Validation, C.L. and F.Z.; write-review and editing, C.L., M.L. and J. Z; write-original manuscript, C. L, M.L.; supervision, J.Z. and X.T. All authors have read and agreed to the published version of the manuscript.

Acknowledgements

We thank Gene Denovo Biotechnology Co. (Guangzhou, China) for its service in RNA-Seq and transcriptome analysis. We thank the Huju Forest Farm in the Chaling district for providing the field test origin and test materials.

Abbreviations

ABA: abscisic acid; GA: gibberellin, ET: ethylene; JA: jasmonic acid; PP2C06:the protein phosphatase 2C gene 56-like; PYL1: PYL1-like gene; GID1B: the GA receptor GID1B-like; ETR2: ET receptor 2-like;EBF2:EIN3-binding F-box protein 1-like; CTR1: serine threonine-protein kinase CTR1-like isoform X1; MYC2: the transcription factor MYC2-like;JAR4-1-2: the jasmonoyl-L-amino acid synthetase JAR4-like; PIP5K6: the phosphatidylinositol 4-phosphate 5-kinase 6-like; DGK1: diacylglycerol kinase 1-like isoform X2; PLC6: phosphoinositide phospholipase C 6-like; DGK2: the diacylglycerol kinase 2; PIP5K6: the 1-phosphatidylinositol-

3-phosphate 5-kinase; FAB1B: FAB1B-like isoform X1; IPK1: inositol-pentakisphosphate 2-kinase-like isoform X2; VIP2: diphosphoinositol-pentakisphosphate kinase VIP2-like；PLC2: phosphoinositide phospholipase C 2-like；GST: Glutathione S-transferase; PX2: glutathione peroxidase; FER: receptor-like protein kinase FERONIA, RBOH: respiratory burst oxidase protein-like; GSTU7: glutathione S-transferase U7-like, AOX1A: mitochondrial alternative oxidase 1d; FER: receptor-like protein kinase HERK 1 isoform; CDPK: Calcium-dependent protein kinase, ACA: calcium-transporting ATPase, CCX: cation/calcium exchanger 1-like; CAM: calmodulin-binding protein; RNS1: extracellular ribonuclease LE-like isoform X1

References

1. Zhang F, Li Z, Zhou J, Gu Y, Tan X. Comparative study on fruit development and oil synthesis in two cultivars of Camellia oleifera. BMC Plant Biol. 2021;21:348.

2. Dong B, Wu B, Hong W, Li X, Li Z, Xue L, et al. Transcriptome analysis of the tea oil camellia (Camellia oleifera) reveals candidate drought stress genes. PLoS ONE. 2017;12:e0181835.

3. Baek S, Choi K, Kim G-B, Yu H-J, Cho A, Jang H, et al. Draft genome sequence of wild Prunus yedoensis reveals massive inter-specific hybridization between sympatric flowering cherries. Genome Biol. 2018;19:127.

4. Lin M, Wang S, Liu Y, Li J, Zhong H, Zou F, et al. 11-Hydrogen cyanamide enhances flowering time in tea oil camellia (Camellia oleifera Abel.). Industrial Crops and Products. 2022;176:114313.

5. He Y, Chen R, Yang Y, Liang G, Zhang H, Deng X, et al. Sugar Metabolism and Transcriptome Analysis Reveal Key Sugar Transporters during Camellia oleifera Fruit Development. IJMS. 2022;23:822.

6. He Y, Song Q, Wu Y, Ye S, Chen S, Chen H. TMT-Based Quantitative Proteomic Analysis Reveals the Crucial Biological Pathways Involved in Self-Incompatibility Responses in Camellia oleifera. IJMS. 2020;21:1987.

7. Lin P, Wang K, Wang Y, Hu Z, Yan C, Huang H, et al. 2 The genome of oil-Camellia and population genomics analysis provide insights into seed oil domestication. Genome Biol. 2022;23:14.

8. Zhou J, Lu M, Yu S, Liu Y, Yang J, Tan X. In-Depth Understanding of Camellia oleifera Self-Incompatibility by Comparative Transcriptome, Proteome and Metabolome. IJMS. 2020;21:1600.

9. Jundao Xu. Health care function and development prospect of Camellia oil[J]. China Fruit and Vegetable 2018.10.

10. He Y, Song Q, Chen S, Wu Y, Zheng G, Feng J, et al. Transcriptome analysis of self- and cross-pollinated pistils revealing candidate unigenes of self-incompatibility in Camellia oleifera. The Journal of Horticultural Science and Biotechnology. 2020;95:19–31.

11. Zhang C-C, Wang L-Y, Wei K, Wu L-Y, Li H-L, Zhang F, et al. Transcriptome analysis reveals self-incompatibility in the tea plant (Camellia sinensis) might be under gametophytic control. BMC Genomics. 2016;17:359.

12. Tan L-Q, Wang L-Y, Wei K, Zhang C-C, Wu L-Y, Qi G-N, et al. Floral Transcriptome Sequencing for SSR Marker Development and Linkage Map Construction in the Tea Plant (Camellia sinensis). PLoS ONE. 2013;8:e81611.

13. Li W, Yang Q, Gu Z, Wu C, Meng D, Yu J, et al. Molecular and genetic characterization of a self-compatible apple cultivar, 'CAU-1.' Plant Science. 2016;252:162–75.

14. Herrera S, Rodrigo J, Hormaza J, Lora J. Identification of Self-Incompatibility Alleles by Specific PCR Analysis and S-RNase Sequencing in Apricot. IJMS. 2018;19:3612.

15. Gibbs PE. Late‐acting self‐incompatibility – the pariah breeding system in flowering plants. New Phytol. 2014;203:717–34.

16. LaDoux T, Friar EA. Late‐Acting Self‐Incompatibility in Ipomopsis tenuifolia (Gray) V. Grant (Polemoniaceae). International Journal of Plant Sciences. 2006;167:463–71.

17. Bagheri M, Ershadi A. Self-incompatibility alleles in Iranian pear cultivars. Biocatalysis and Agricultural Biotechnology. 2020;27:101672.

18. Ma J-Z, Wang H-J, Wang D-S, Li X-Y, Liu J-Z, Xiao X, et al. Self-compatibility of Crataegus pinnatifida Bge. 'Zizhenzhu' is associated with the mutation of a pistil-part non-S factor. Scientia Horticulturae. 2020;268:109362.

19. Li Y, Wu J, Wu C, Yu J, Liu C, Fan W, et al. A mutation near the active site of S-RNase causes self-compatibility in S-RNase-based self-incompatible plants. Plant Mol Biol. 2020;103:129–39.

20. Yang Q, Meng D, Gu Z, Li W, Chen Q, Li Y, et al. Apple S -RNase interacts with an actin-binding protein, MdMVG, to reduce pollen tube growth by inhibiting its actin-severing activity at the early stage of self-pollination induction. Plant J. 2018;95:41–56.

21. Li T, Long S, Li M, Bai S, Zhang W. Determination S-Genotypes and Identification of Five Novel S-RNase Alleles in Wild Malus Species. Plant Mol Biol Rep. 2012;30:453–61.

22. Wu J, Li M, Li T. Genetic Features of the Spontaneous Self-Compatible Mutant, 'Jin Zhui' (Pyrus bretschneideri Rehd.). PLoS ONE. 2013;8:e76509.

23. Liang M, Cao Z, Zhu A, Liu Y, Tao M, Yang H, et al. Evolution of self-compatibility by a mutant Sm-RNase in citrus. Nat Plants. 2020;6:131–42.

24. Wu L, Williams JS, Sun L, Kao T. Sequence analysis of the Petunia inflata S ‐locus region containing 17 S ‐Locus F ‐Box genes and the S ‐RNase gene involved in self ‐incompatibility. Plant J. 2020;104:1348–68.

25. Chen X, Hao S, Wang L, Fang W, Wang Y, Li X. Late-acting self-incompatibility in tea plant (Camellia sinensis). Biologia. 2012;67:347–51.

26. Ford CS, Wilkinson MJ. Confocal observations of late-acting self-incompatibility in Theobroma cacao L. Sex Plant Reprod. 2012;25:169–83.

27. 10655239.pdf.

28. Chen J, Wang P, de Graaf BHJ, Zhang H, Jiao H, Tang C, et al. Phosphatidic Acid Counteracts S-RNase Signaling in Pollen by Stabilizing the Actin Cytoskeleton. Plant Cell. 2018;30:1023–39.

29. Wilkins KA, Bancroft J, Bosch M, Ings J, Smirnoff N, Franklin-Tong VE. Reactive Oxygen Species and Nitric Oxide Mediate Actin Reorganization and Programmed Cell Death in the Self-Incompatibility Response of Papaver. Plant Physiology. 2011;156:404–16.

30. Serrano I, Romero-Puertas MC, Sandalio LM, Olmedilla A. The role of reactive oxygen species and nitric oxide in programmed cell death associated with self-incompatibility. Journal of Experimental Botany. 2015;66:2869–76.

31. Del Duca S, Aloisi I, Parrotta L, Cai G. Cytoskeleton, Transglutaminase and Gametophytic Self-Incompatibility in the Malinae (Rosaceae). IJMS. 2019;20:209.

32. Qin N, Gao Y, Cheng X, Yang Y, Wu J, Wang J, et al. Genome-wide identification of CLE gene family and their potential roles in bolting and fruit bearing in cucumber (Cucumis sativus L.). BMC Plant Biol. 2021;21:143.

33. Sheng H, Zhang S, Wei Y, Chen S. Exogenous Application of Low-Concentration Sugar Enhances Brassinosteroid Signaling for Skotomorphogenesis by Promoting BIN2 Degradation. IJMS. 2021;22:13588.

34. Shi D, Tang C, Wang R, Gu C, Wu X, Hu S, et al. Transcriptome and phytohormone analysis reveals a comprehensive phytohormone and pathogen defence response in pear self-/cross-pollination. Plant Cell Rep. 2017;36:1785–99.

35. Meng D, Gu Z, Li W, Wang A, Yuan H, Yang Q, et al. Apple MdABCF assists in the transportation of S -RNase into pollen tubes. Plant J. 2014;78:990–1002.

36. Kaya H, Nakajima R, Iwano M, Kanaoka MM, Kimura S, Takeda S, et al. Ca 2+ -Activated Reactive Oxygen Species Production by Arabidopsis RbohH and RbohJ Is Essential for Proper Pollen Tube Tip Growth. Plant Cell. 2014;26:1069–80.

37. Li C, Zhang N, Guan B, Zhou Z, Mei F. Reactive oxygen species are involved in cell death in wheat roots against powdery mildew. Journal of Integrative Agriculture. 2019;18:1961–70.

38. Yoon GM, Dowd PE, Gilroy S, McCubbin AG. Calcium-Dependent Protein Kinase Isoforms in Petunia Have Distinct Functions in Pollen Tube Growth, Including Regulating Polarity. The Plant Cell. 2006;18:867–78.

39. Entani T, Kubo K, Isogai S, Fukao Y, Shirakawa M, Isogai A, et al. Ubiquitin-proteasome-mediated degradation of S-RNase in a solanaceous cross-compatibility reaction. Plant J. 2014;78:1014–21.

40. Abdallah D, Baraket G, Perez V, Ben Mustapha S, Salhi-Hannachi A, Hormaza JI. Analysis of Self-Incompatibility and Genetic Diversity in Diploid and Hexaploid Plum Genotypes. Front Plant Sci. 2019;10:896.

41. Honsho C, Ushijima K, Anraku M, Ishimura S, Yu Q, Gmitter FG, et al. Association of T2/S-RNase With Self-Incompatibility of Japanese Citrus Accessions Examined by Transcriptomic, Phylogenetic, and Genetic Approaches. Front Plant Sci. 2021;12:638321.

42. Qin XM, Zhang Y, Liu YJ, Guo DN, Li HM. Molecular mechanisms underlying the participation of Ribonuclease T2 gene into self-incompatibility of Citrus grandis var. Shatianyu Hort. Cell Mol Biol (Noisy-le-grand). 2018;64.

43. MacIntosh GC, Hillwig MS, Meyer A, Flagel L. RNase T2 genes from rice and the evolution of secretory ribonucleases in plants. Mol Genet Genomics. 2010;283:381–96.

44. Liang M, Yang W, Su S, Fu L, Yi H, Chen C, et al. Genome-wide identification and functional analysis of S-RNase involved in the self-incompatibility of citrus. Mol Genet Genomics. 2017;292:325–41.

45. Luhtala N, Parker R. T2 Family ribonucleases: ancient enzymes with diverse roles. Trends in Biochemical Sciences. 2010;35:253–9.

46. Lu B, Chen L, Hao J, Zhang Y, Huang J. Comparative transcription profiles reveal that carbohydrates and hormone signalling pathways mediate flower induction in Juglans sigillata after girdling. Industrial Crops and Products. 2020;153:112556.

47. Manghwar H, Hussain A, Ali Q, Liu F. Brassinosteroids (BRs) Role in Plant Development and Coping with Different Stresses. IJMS. 2022;23:1012.

48. Zhang J, Qian J-Y, Bian Y-H, Liu X, Wang C-L. Transcriptome and Metabolite Conjoint Analysis Reveals the Seed Dormancy Release Process in Callery Pear. IJMS. 2022;23:2186.

49. Song Y, Feng L, Alyafei MAM, Jaleel A, Ren M. Function of Chloroplasts in Plant Stress Responses. IJMS. 2021;22:13464.

50. Lu M, Zhou J, Liu Y, Yang J, Tan X. CoNPR1 and CoNPR3.1 are involved in SA‐ and MeSA‐ mediated growth of the pollen tube in Camellia oleifera. Physiologia Plantarum. 2021;172:2181–90.

51. Zakharova EV, Timofeeva GV, Fateev AD, Kovaleva LV. Caspase-like proteases and the phytohormone cytokinin as determinants of S-RNAse–based self-incompatibility–induced PCD in Petunia hybrida L. Protoplasma. 2021;258:573–86.

52. Liu C, Xiao P, Jiang F, Wang S, Liu Z, Song G, et al. Exogenous gibberellin treatment improves fruit quality in self-pollinated apple. Plant Physiology and Biochemistry. 2022;174:11–21.

53. Gu Z, Li W, Doughty J, Meng D, Yang Q, Yuan H, et al. A gamma‐thionin protein from apple, MdD1, is required for defence against S‐RNase‐induced inhibition of pollen tube prior to self/non‐self recognition. Plant Biotechnol J. 2019;17:2184–98.

54. Kucera B, Cohn MA, Leubner-Metzger G. Plant hormone interactions during seed dormancy release and germination. Seed Sci Res. 2005;15:281–307.

55. Chang E, Deng N, Zhang J, Liu J, Chen L, Zhao X, et al. Proteome-Level Analysis of Metabolism- and Stress-Related Proteins during Seed Dormancy and Germination in Gnetum parvifolium. J Agric Food Chem. 2018;66:3019–29.

56. Liu J, Chen L-Y, Zhou P, Liao Z, Lin H, Yu Q, et al. Sex biased expression of hormone related genes at early stage of sex differentiation in papaya flowers. Hortic Res. 2021;8:147.

57. Baker RP, Hasenstein KH, Zavada MS. Hormonal Changes after Compatible and Incompatible Pollination in Theobroma cacao L. HortSci. 1997;32:1231–4.

58. Hwang I, Sheen J, Müller B. Cytokinin Signaling Networks. Annu Rev Plant Biol. 2012;63:353–80.

59. Guo Z, Yuan X, Li L, Zeng M, Yang J, Tang H, et al. Genome-Wide Analysis of the ATP-Binding Cassette (ABC) Transporter Family in Zea mays L. and Its Response to Heavy Metal Stresses. IJMS. 2022;23:2109.

60. Niu L, Li H, Song Z, Dong B, Cao H, Liu T, et al. The functional analysis of ABCG transporters in the adaptation of pigeon pea (Cajanus cajan) to abiotic stresses. PeerJ. 2021;9:e10688.

61. Qu H, Guan Y, Wang Y, Zhang S. PLC-Mediated Signaling Pathway in Pollen Tubes Regulates the Gametophytic Self-incompatibility of Pyrus Species. Front Plant Sci. 2017;8:1164.

62. Xu J, Brearley CA, Lin W-H, Wang Y, Ye R, Mueller-Roeber B, et al. A Role of Arabidopsis Inositol Polyphosphate Kinase, AtIPK2 α , in Pollen Germination and Root Growth. Plant Physiology. 2005;137:94–103.

63. Zhou, Liu, Chen, Liu, Wang, Zheng, et al. Comparative Transcriptome Analysis Reveals the Cause for Accumulation of Reactive Oxygen Species During Pollen Abortion in Cytoplasmic Male-Sterile Kenaf Line 722HA. IJMS. 2019;20:5515.

64. Baxter A, Mittler R, Suzuki N. ROS as key players in plant stress signalling. Journal of Experimental Botany. 2014;65:1229–40.

65. Tiwari BS, Belenghi B, Levine A. Oxidative Stress Increased Respiration and Generation of Reactive Oxygen Species, Resulting in ATP Depletion, Opening of Mitochondrial Permeability Transition, and Programmed Cell Death. Plant Physiology. 2002;128:1271–81.

66. Wu C, Gu Z, Li T, Yu J, Liu C, Fan W, et al. The apple MdPTI1L kinase is phosphorylated by MdOXI1 during S-RNase-induced reactive oxygen species signaling in pollen tubes. Plant Science. 2021;305:110824.

67. Sun C-Q, Chen F-D, Teng N-J, Yao Y-M, Shan X, Dai Z-L. Transcriptomic and proteomic analysis reveals mechanisms of low pollen-pistil compatibility during water lily cross breeding. BMC Plant Biol. 2019;19:542.

68. Wang X, Liu S, Sun H, Liu C, Li X, Liu Y, et al. Production of reactive oxygen species by PuRBOHF is critical for stone cell development in pear fruit. Hortic Res. 2021;8:249.

69. Hiscock S, Bright J, McInnis SM, Desikan R, Hancock JT. Signaling on the Stigma: Potential New Roles for ROS and NO in Plant Cell Signaling. Plant Signaling & Behavior. 2007;2:23–4.

70. Wang C-L, Wu J, Xu G-H, Gao Y, Chen G, Wu J-Y, et al. S-RNase disrupts tip-localized reactive oxygen species and induces nuclear DNA degradation in incompatible pollen tubes of Pyrus pyrifolia. Journal of Cell Science. 2010;123:4301–9.

71. Qin Y, Yang Z. Rapid tip growth: Insights from pollen tubes. Seminars in Cell & Developmental Biology. 2011;22:816–24.

72. Konrad KR, Wudick MM, Feijó JA. Calcium regulation of tip growth: new genes for old mechanisms. Current Opinion in Plant Biology. 2011;14:721–30.

73. Peer LA. Self-Incompatibility Patterns and Signal Transduction. In: Hakeem KR, Rehman RU, Tahir I, editors. Plant signaling: Understanding the molecular crosstalk. New Delhi: Springer India; 2014. p. 327–43.

74. Xu C, Li M, Wu J, Guo H, Li Q, Zhang Y, et al. Identification of a canonical SCFSLF complex involved in S-RNase-based self-incompatibility of Pyrus (Rosaceae). Plant Mol Biol. 2013;81:245–57.

75. Sun L, Williams JS, Li S, Wu L, Khatri WA, Stone PG, et al. S-Locus F-Box Proteins Are Solely Responsible for S-RNase-Based Self-Incompatibility of Petunia Pollen. Plant Cell. 2018;30:2959–72.

76. Romero C, Vilanova S, Burgos L, Martnez-Calvo J, Vicente M, Llcer G, et al. Analysis of the S-locus structure in Prunus armeniaca L. Identification ofS-haplotype specific S-RNase and F-box genes. Plant Mol Biol. 2004;56:145–57.

77. Seth R, Bhandawat A, Parmar R, Singh P, Kumar S, Sharma R. Global Transcriptional Insights of Pollen-Pistil Interactions Commencing Self-Incompatibility and Fertilization in Tea [Camellia sinensis (L.) O. Kuntze]. IJMS. 2019;20:539.

78. Tan XF, Yuan DY, Yuan J, et al. An Elite Varirty: Camellia oleifera ‘Huashuo’. Scientia Silvae Sinm, 2011;47,12.

79. Yuan DY, Tan XF, Yuan J, et al. An Elite Varirty: Camellia oleifera ‘Huajin’. Scientia Silvae Sinm, 2012;48,2.

80. Chen S, Zhou Y, Chen Y, Gu J, Biotechnology H. fastp: an ultra-fast all-in-one FASTQ preprocessor. :12.

81. Kim D, Langmead B, Salzberg SL. HISAT: a fast spliced aligner with low memory requirements. Nat Methods. 2015;12:357–60.

82. Pertea M, Pertea GM, Antonescu CM, Chang T-C, Mendell JT, Salzberg SL. StringTie enables improved reconstruction of a transcriptome from RNA-seq reads. Nat Biotechnol. 2015;33:290–5.

83. Pertea M, Kim D, Pertea GM, Leek JT, Salzberg SL. Transcript-level expression analysis of RNA-seq experiments with HISAT, StringTie and Ballgown. Nat Protoc. 2016;11:1650–67.

84.Kanehisa, M. and Goto, S.; KEGG: Kyoto Encyclopedia of Genes and Genomes. Nucleic Acids Res. 28, 27-30 (2000).

85. Love MI, Huber W, Anders S. Moderated estimation of fold change and dispersion for RNA-seq data with DESeq2. 2014;:22.

86. Robinson MD, McCarthy DJ, Smyth GK. edgeR: a Bioconductor package for differential expression analysis of digital gene expression data. Bioinformatics. 2010;26:139–40.

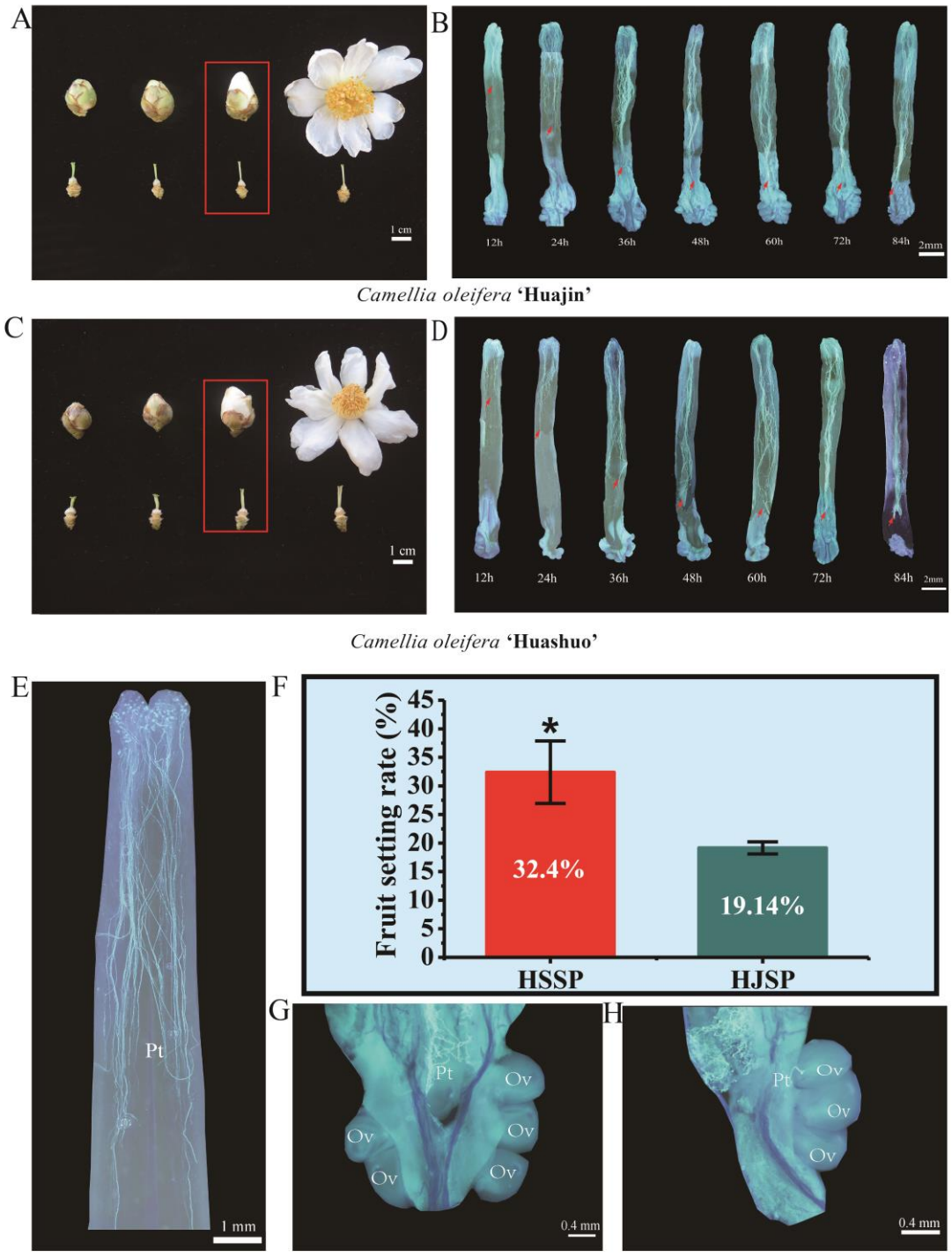

Figure 1 Pollen tube growth from 12h to 84h in pistil after self-pollination and fruiting setting rates in *Camellia oleifera* HJ and HS. (**A**)Flower bud at different development stages of HJ; (**B**) Pollen tube growth from 12h to 84h in the pistil after self-pollination in HJ (40×); (**C**) Flower bud at different development stages of HS; (**D**) Pollen tube growth from 12h to 84h in the pistil after self-pollination in HS(40×); (**E**) Normal growth pollen tube after self-pollinated in HS; (**F**) Fruit setting rate in *Camellia oleifera* HJ and HS; .(G-H) Pollen tube growth to the ovary successfully 60h after self-pollination. Pt=pollen tube, Ov=ovary.

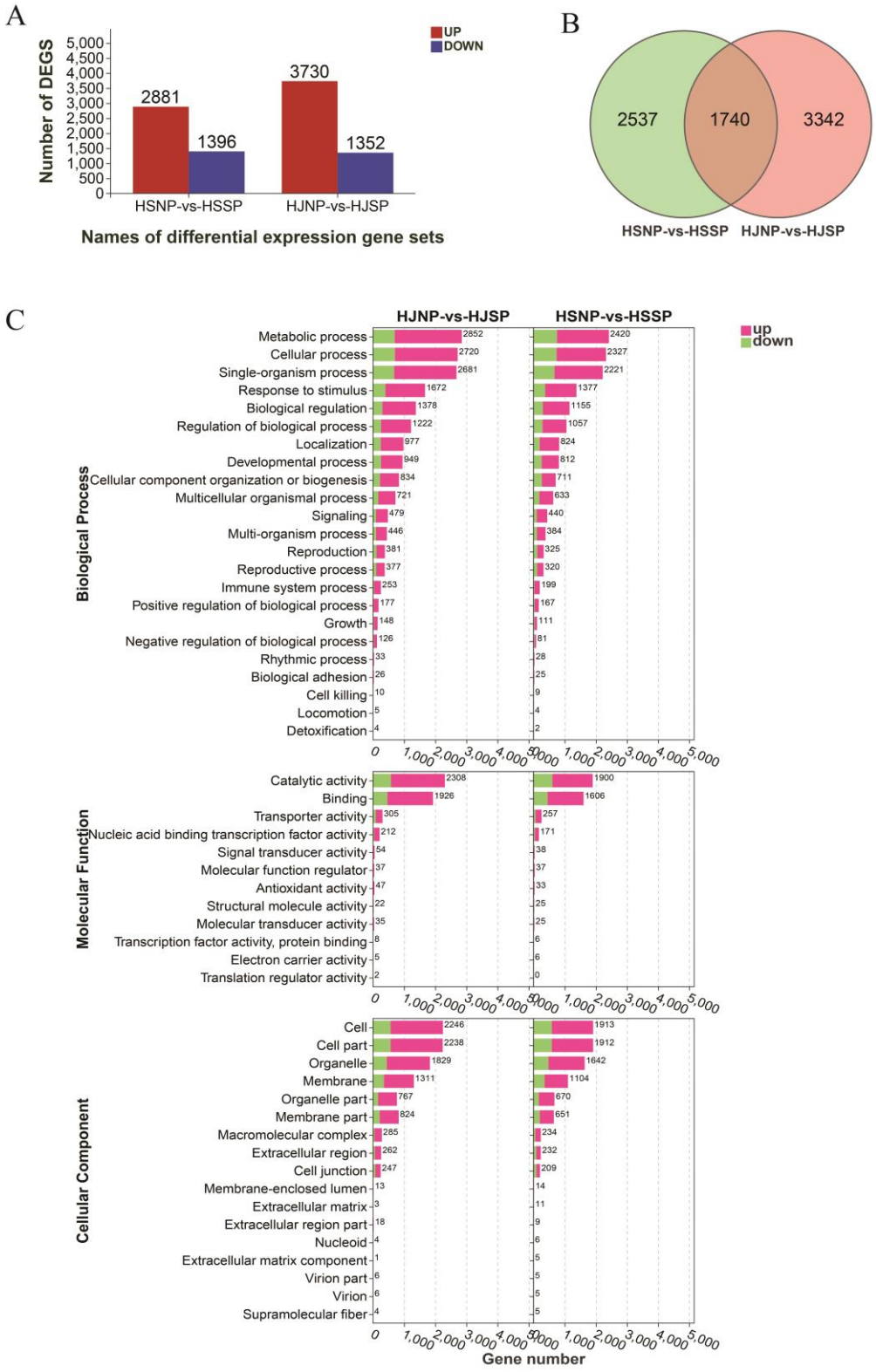

Figure 2 Analysis of differentially expressed transcripts in self- and non-pollinated ovary of Camellia oleifera. (**A**)Number of up- and down- regulated DEGs in the two groups; (**B**)Venn diagram showing all DEGs numbers of two gene sets; (**C**) GO function annotation of the two cultivars ovary transcriptome of *Camellia oleifera* 'Huajin' and 'Huashuo'.

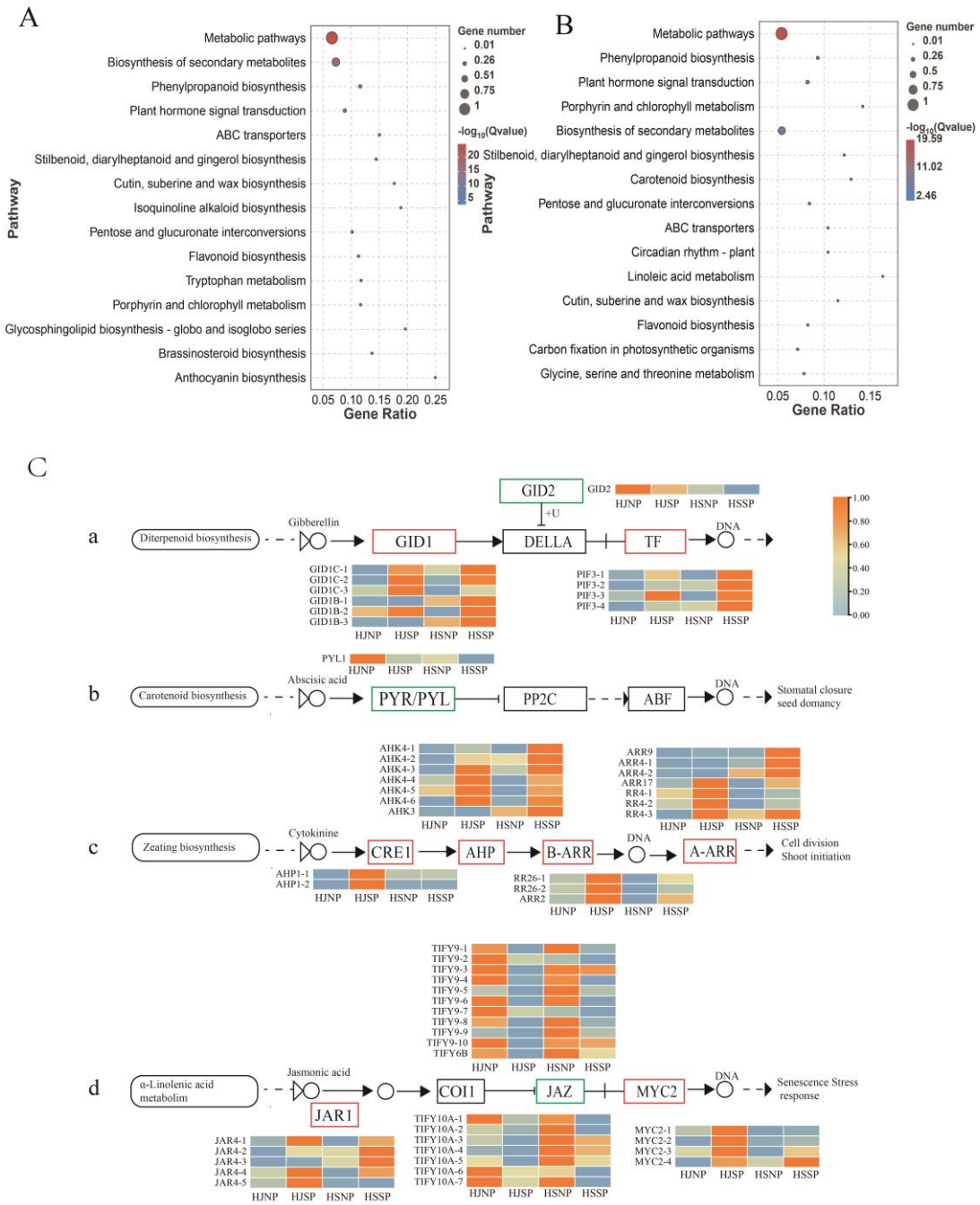

Figure 4 KEGG enrichment pathway anysis of DEGs in in self- and non-pollinated ovary of *Camellia oleifera*. **(A)** Top 15 KEGG Pathways annotation of DEGs in HSNP_HSSP gene set. (**B**) Top 15 KEGG Pathways annotation of DEGs in HSNP_HSSP gene set.**(C)**The differentially expressed genes in hormone signaling pathways in response to self-incompatibility in *Camellia oleifera* 'Huajin' and 'Huashuo'

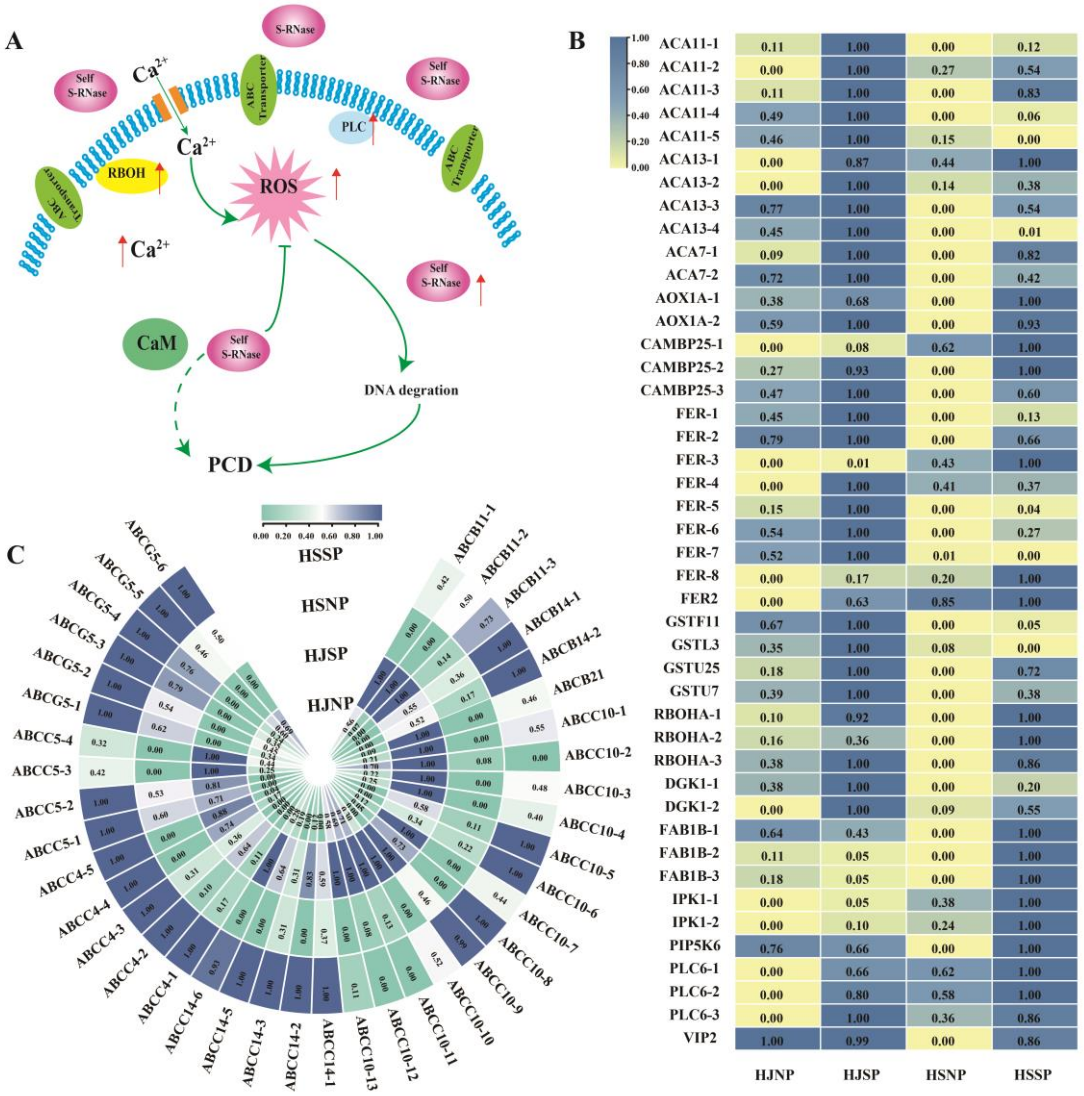

Figure 4. Expression profiles of gene in ABC transporters, Phosphatidylinositol signaling system, ROS and Ca^{2+} signaling pathway. (**A**) Simplified representation of most relevant molecule found to be involved in SI. (**B**) Comparison of expression patterns of key genes related to Phosphatidylinositol signaling system, ROS and Ca^{2+} signaling pathway in self- and non- pollinated ovary of Camellia oleifera. yellow and blue indicate indicate relative decreases and increases in expression (log_2 fold change). The annotation of these genes are exhibited in Table S2. ACA: Calcium-transporting ATPase; CAMBP25: calmodulin-binding protein 25; FER: receptor-like protein kinase FERONIA; GSTF: glutathione S-transferase; RBOHA: Respiratory burst oxidase protein like; DGK: diacylglycerol kinase 1-like isoform X2; FAB1B: 1-phosphatidylinositol-3-phosphate 5-kinase FAB1B-like isoform X1; IPK: inositol-pentakisphosphate 2-kinase; PIP5K6: phosphatidylinositol 4-phosphate 5-kinase 6-like; PLC6: phosphoinositide phospholipase C 6-like; VIP:nositol hexakisphosphate and diphosphoinositol-pentakisphosphate kinase VIP2-like. (**C**) Comparison of expression patterns of key genes related to ABC transporter pathway in self- and non- pollinated ovary of Camellia *oleifera*. green and blue indicate indicate relative decreases and increases in expression (log_2 fold change). The annotation of these genes are exhibited in Table S3. ABCB: ABC transporter B family member; ABCC: ABC transporter C family member; ABCG: ABC transporter G family member.

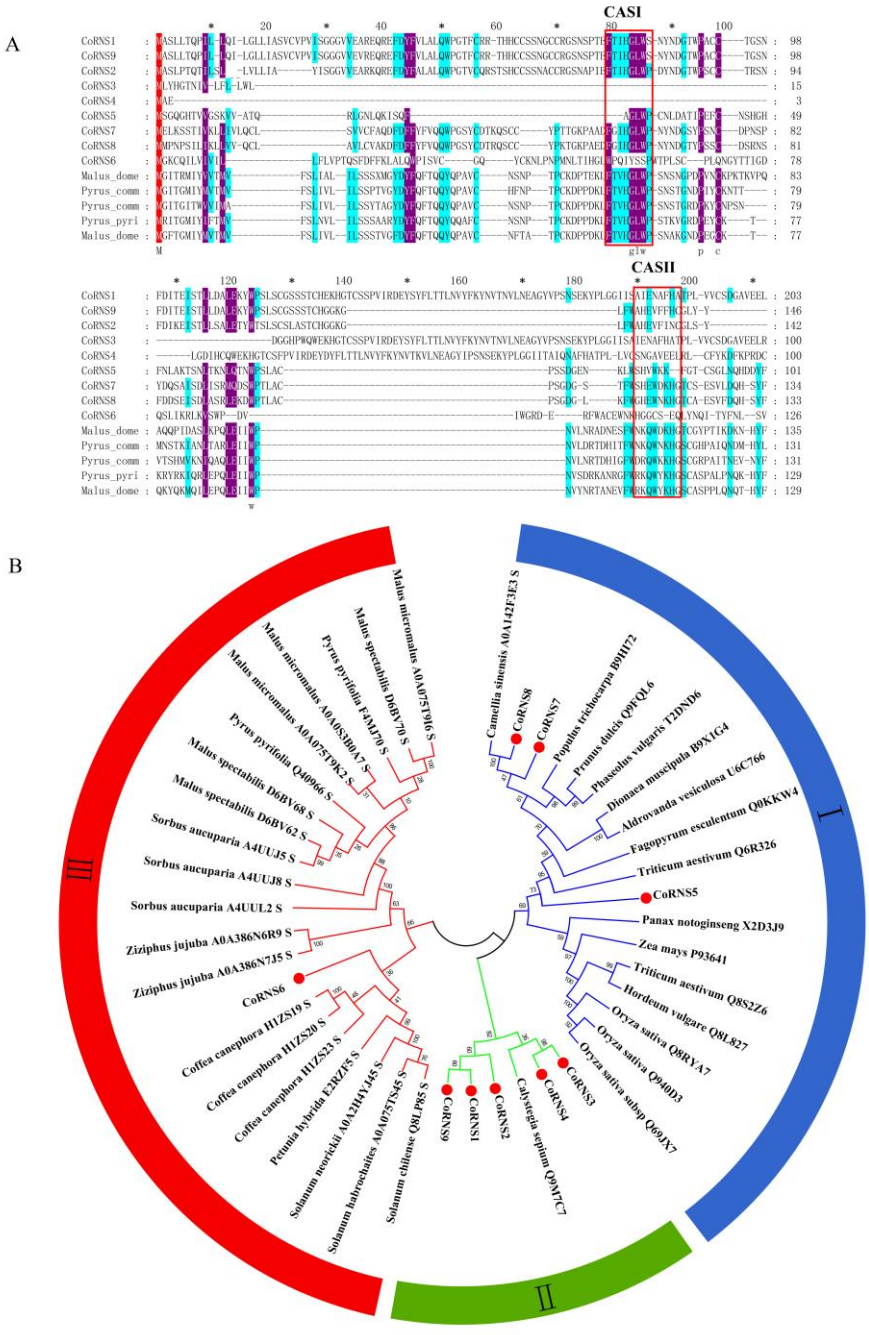

Figure 5 Analysis of the 9 RNase T2 genes from *Camellia oleifera*. (**A**) Phylogenetic analysis of the 9 RNase T2 genes ;(**B**) Amino-acid sequence alignment of 9 RNase T2 genes and the S-RNase from other species.

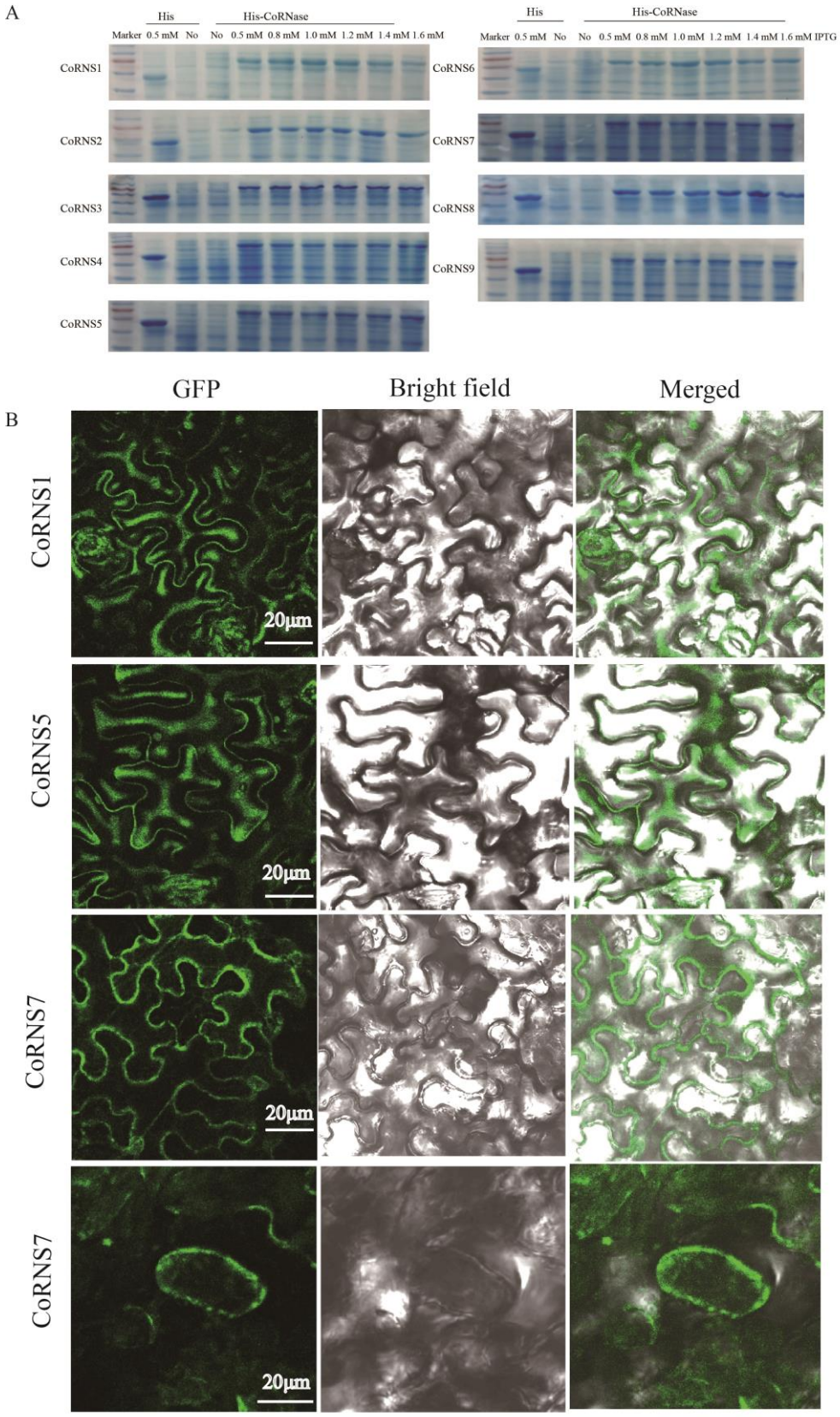

Figure 6 The protein expression analysis of the RNase T2 genes. (**A**) The prokaryotic expression analysis of 9 RNase T2 genes. (**B**)The subcellular localization of CoRNS1, CoRNS5, and CoRNS7.

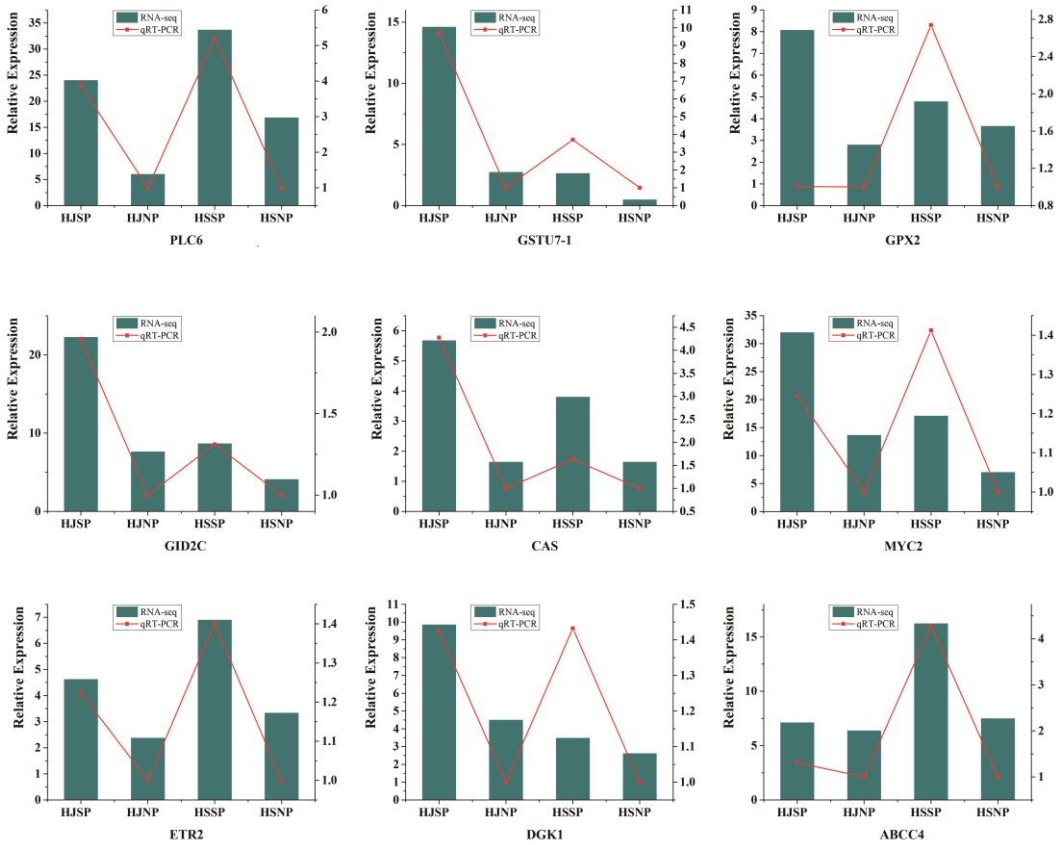

Figure 7. Quantitative qRT-PCR validation of 9 DEGs identified related to self-incompatibility.

Table 1. Summary of Sequence reads and Unigenes for twelve RNA samples from De novo assembly

Sample	Raw_reads(Mb)	Clean_reads(Mb)	Clean_bases(Gb)	Q20	Q30	Unique_map	Multi_map	Total_map
HJNP-1	66.78	66.50	9.92	98.00%	94.16%	39267036 (59.08%)	21089363 (31.73%)	60356399 (90.81%)
HJNP-2	69.22	69.02	10.10	98.10%	94.41%	40222163 (58.31%)	21918936 (31.78%)	62141099 (90.09%)
HJNP-3	61.92	61.71	9.02	97.87%	93.82%	36100019 (58.54%)	19422333 (31.50%)	55522352 (90.04%)
HJSP-1	47.98	47.89	7.15	98.33%	94.74%	28096446 (58.71%)	15250400 (31.87%)	43346846 (90.57%)
HJSP-2	50.43	50.33	7.52	98.15%	94.26%	29748589 (59.14%)	15790304 (31.39%)	45538893 (90.53%)
HJSP-3	52.69	52.60	7.86	98.07%	94.04%	30664191 (58.34%)	16592787 (31.57%)	47256978 (89.90%)
HSNP-1	61.12	60.95	9.09	97.94%	93.91%	38592078 (63.37%)	18130734 (29.77%)	56722812 (93.14%)
HSNP-2	62.36	62.18	9.27	97.77%	93.62%	39226394 (63.13%)	18632072 (29.98%)	57858466 (93.11%)
HSNP-3	72.42	72.21	10.76	97.95%	94.07%	44810287 (62.10%)	22744249 (31.52%)	67554536 (93.62%)
HSSP-1	44.88	44.80	6.70	98.28%	94.59%	28700957 (64.11%)	13046307 (29.14%)	41747264 (93.25%)
HSSP-2	61.69	61.58	9.21	98.12%	94.19%	39366886 (63.97%)	17537945 (28.50%)	56904831 (92.47%)
HSSP-3	57.18	57.09	8.64	98.26%	94.52%	36229624 (63.51%)	16581192 (29.07%)	52810816 (92.58%)

Table 2. characteristics of RNase T2 genes from Camellia oil tree（*camellia oleifera*）

name	ID	Length of CDS	Amino acid	Molecular weight	PI	Signal peptide
*Co*RNS1	oil_tea_GLEAN_10114714	748	315	34.82	5.6	yes
*Co*RNS2	oil_tea_GLEAN_10391745	429	142	15.65	6.02	yes
*Co*RNS3	oil_tea_GLEAN_10141428	480	159	17.75	5.39	yes
*Co*RNS4	oil_tea_GLEAN_10391744	448	143	16.0	4.94	no
*Co*RNS5	oil_tea_GLEAN_10004004	480	159	17.39	8.6	no
*Co*RNS6	oil_tea_GLEAN_10401437	753	250	28.39	8.77	yes
*Co*RNS7	oil_tea_GLEAN_10185682	684	227	24.97	4.59	yes
*Co*RNS8	oil_tea_GLEAN_10400090	717	262	26.54	5.42	yes
*Co*RNS9	oil_tea_GLEAN_10340465	457	146	16.1	5.78	yes

Additional Files

Additional file 1: Figure S1. The prokaryotic expression analysis of 9 RNase T2 genes.

Additional file 2: Table S1. the unannotated unigenes in the transcriptome data.

Additional file 3: Table S2. DEGs involved in ABC transporters in two comparisons.

Additional file 4: Table S3. DEGs related to the phosphatidylinositol signaling system in two comparisons.

Additional file 5: Table S4. Gene-specific primers used in RT-qPCR.